INFLUENCE OF STRUCTURAL PARAMETERS ON MECHANICAL PROPERTIES OF R6M5 STEEL UNDER THE CONDITIONS OF STRENGTHENING SURFACE TREATMENT

L.I. MARKASHOVA, Yu.N. TYURIN, O.V. KOLISNICHENKO, M.L. VALEVICH and **D.G. BOGACHEV**

E.O. Paton Electric Welding Institute, NASU

11 Bozhenko Str., 03680, Kiev, Ukraine. E-mail: office@paton.kiev.ua

The work is devoted to investigation of structural-phase changes in surface layers of high-speed steel R6M5 after strengthening pulsed-plasma surface treatment in various modes and influence of forming structure parameters on tool performance. As a result of comprehensive investigations and calculation-analytical prediction of strength properties, fracture toughness coefficient and crack resistance of surfaces, strengthened in various technological modes, it was established that optimum properties of subsurface layers are ensured at recommended modes of pulsed-plasma surface treatment, increasing the total strength level by 25 %, compared with base metal due to refinement of grain structure (by 1.5 to 2 times), increase of the contribution of substructural, grain, dislocation and dispersion strengthening mechanism. Here, the level of local inner stresses in the treated layer is equal to ~0.018 to 0.44 of the theoretical strength of material that is not dangerous in terms of crack formation, because of the absence of abrupt gradients as to inner stresses and uniformly increased dislocation density (10^{11}–2.10^{11} cm^{-2}) compared to base metal. It is shown that at a significant strengthening of treated layers of high-speed steel, the value of fracture toughness coefficient is by 15 % higher compared to base metal. Thus, application of recommended modes of pulsed-plasma surface treatment leads to modifying the structural-phase state of the surface layer and improvement of its mechanical properties. 31 Ref., 9 Figures.

Tool steel R6M5 is designed for operation under the conditions of high contact loads and temperatures, and this, as a rule, are metal-working tools, where the item working layer is exposed to the most intensive wear. Considering the complicated service conditions, improvement of the set of physico-mechanical properties of this layer by recrystallization and structure modification is of interest. Preliminary studies showed [1–4] that the most significant changes in the surface layer structure are observed at application of concentrated heat sources: laser, electron beam, plasma, etc. Technology of pulsed-plasma treatment (PPT) developed at PWI is also used with the same purpose [5–7].

Technology of steel PPT is based on the impact of concentrated plasma flows in the pulsed mode on material surface, leading to increase of hardness, grain refinement, structure fragmentation and elimination of clusters of coarse carbide particles, as well as formation of martensite with excess carbon content (because of partial disso-

lution of carbides) and alloying elements in the treated layer [7–18]. At present, however, the information on the influence of various technological parameters of PPT on structural-phase transformations, and of structural parameters — on service characteristics (properties of strength, ductility and crack resistance) of treated items is limited.

The objective of this work is experimental study of the structure and calculation-analytical prediction of properties in surface layers of samples from R6M5 steel after PPT in various modes.

Materials and investigation procedure. Samples from R6M5 steel (GOST 19265–73) were first subjected to standard heat treatment — quenching (T_q = 1200–1230 °C) and tempering (T_t = 540–560 °C). PPT (impact duration t_p ~ ~ 0.5 s) was conducted in the following modes: I — direct impact of pulsed electric discharge (distance H = 60 mm, heat flow q ~ ~ $0.7 \cdot 10^5$ W/cm^2), and II — indirect action of electric discharge (H = 30 mm, q ~ ~ $0.5 \cdot 10^5$ W/cm^2).

Investigations of structural-phase state of surface of samples, treated by PPT, were conducted using a comprehensive procedural approach, in-

cluding optical metallography (the Union Versamet-2, Japan), scanning electron microscopy (Philips SEM-515, Holland) and JEOL transmission microdiffraction electron microscopy JEM-200 CX (Japan) with accelerating voltage of 200 kV. Obtained experimental data allowed performance of calculation-analytical assessment of a concrete (differentiated) contribution of individual structural parameters (phase composition, size of grains, subgrains, dislocation density, etc.) into the change of total (integral) values of mechanical characteristics of strength σ_y, fracture toughness coefficient (stress intensity factor K_{1c}) and crack resistance ($\tau_{l.in}/\tau_{theor}$).

Integral values of yield limit $\Sigma\sigma_y$ of R6M5 steel after PPT in various modes were calculated using Hall−Petch, Zeger, Orowan and other dependencies [19−28], allowing assessment of differentiated contribution $\Delta\sigma$ of specific structural-phase parameters into $\Sigma\sigma_y$.

Fracture toughness of treated layer material was determined from dependence $K_{1c} = (2E\sigma_y\delta_{cr})^{1/2}$ [29], where E is the Young's modulus; σ_y is the calculated strengthening, MPa; δ_{cr} is the crack opening displacement, equal to average size of subgrains, μm.

Level of local internal stress $\tau_{l.in}$, i.e potential sources of crack initiation and propagation in the strengthened layer, was calculated using dependence $\tau_{l.in} = Gbh\rho/[\pi(1-\nu)$ [30, 31], where G is the shear modulus, MPa; b is the Burgers vector; h is the foil thickness, equal to $2\cdot10^{-5}$ cm; ν is the Poisson's ratio; ρ is the dislocation density, cm^{-2}.

Investigation results. It is experimentally established that base metal structure (grain size number D_{gr}, μm; volume fraction of structural components V_{fr}, %) at depth $\delta > 100$ μm from treated surfaces (Figure 1, layers 4 and 7) consists of fine-needled martensite ($D_{gr} \sim 2.5−10$ μm, $V_{fr} = 70$ %), residual austenite ($D_{gr} \sim 2.5−10$ μm, $V_{fr} = 20$ %) and carbides ($D_{gr} = 0.5−20$ μm, $V_{fr} = 10$ %) (Figure 2). Integral microhardness of steel was $HV0.05 \sim 7010$ MPa (Figure 3). Volume fraction of strengthening carbide particles located in grain volumes $V_{fr} = 8$ %. Total fraction of carbides in the material is 18 %.

After PPT (mode I) a surface-melted layer 1 ($\delta \leq 5$ μm) forms on sample surface (Figure 1, a). Below is layer 2 ($\delta \leq 40$ μm), where coarsening of austenitic-martensitic structural components by 2−2.5 times ($D_{gr} \sim 5−25$ μm) and overall lowering by 20 % of total microhardness ($HV0.05 \leq 6200$ MPa) take place (see Figures 2 and 3). This is exactly why zones of microcrack initiation were found in surface-melted layer 1 ($\delta \leq 5$ μm) along the boundaries of residual austenite and
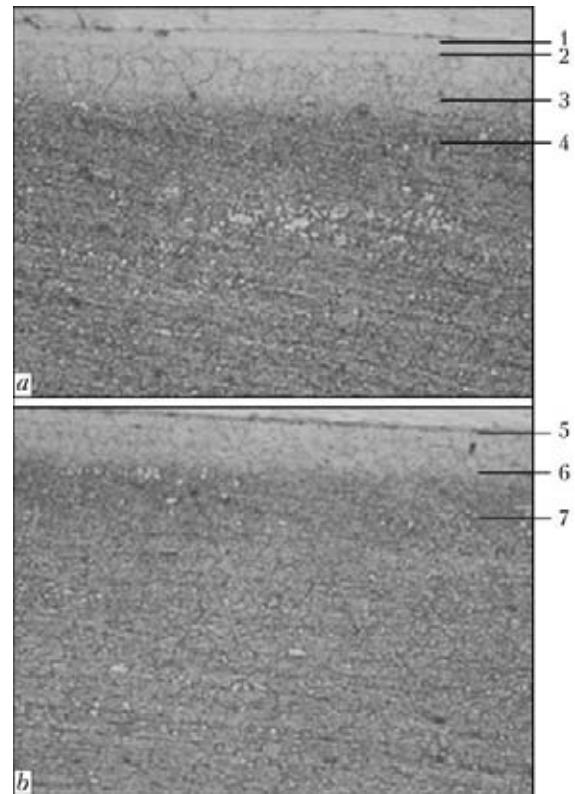
Figure 1. Microstructure (×500) of samples from R6M5 steel after PPT in modes I (*a*) and II (*b*) (changes by depth of treated surface down to base metal): 1 — surface-melted; 2, 5 — structured; 3, 6 — transition layer; 4, 7 — base metal

carbides, using optical and transmission microscopy.

PPT of samples in mode II leads to 1.5 to 2 times refinement of austenitic-martensitic structural components ($D_{gr} \sim 1.5−5$ μm) in modified layer 5 ($\delta = 0−40$ μm) (Figure 2). 20 % increase of total microhardness ($HV0.05 \leq 9200$ MPa) was also found (Figure 3). No cracking in surface layer 5 after PPT in mode II was noted. The observed refinement of granular structure in the layer of high-speed steel R6M5 at PPT in mode II is due to austenite alloying at dissolution of secondary carbides. Primary carbides do not dissolve and inhibit austenite grain growth, thus
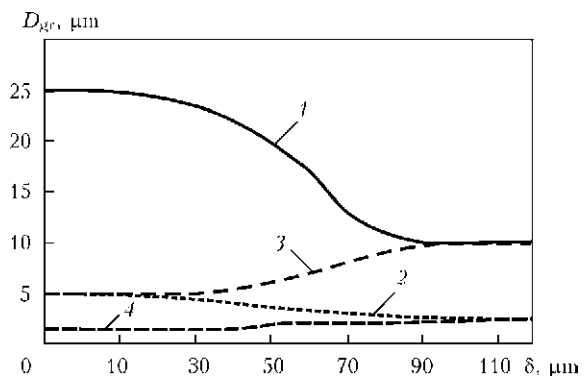
Figure 2. Change of structure dimensions D_{gr} (austenite and martensite) by depth δ of treated layers of samples from R6M5 steel after PPT: *1, 2* — mode I; *3, 4* — mode II

HV, MPa
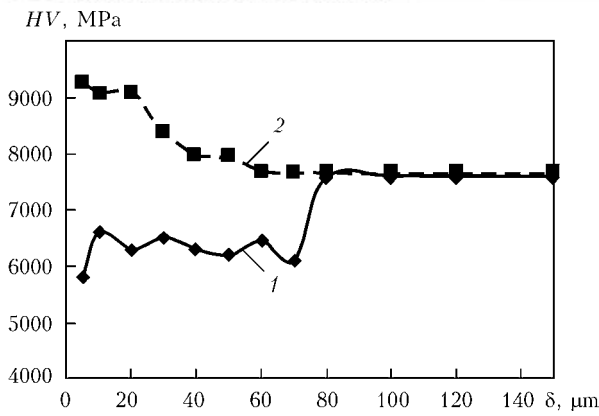
Figure 3. Change of microhardness HV by depth δ of treated layers of samples from steel R6M5 after PPT: *1* — mode I; *2* — mode II

leading to preservation of disperse structure of R6M5 steel at heating close to melting temperature.

Investigations of the change of chemical element concentration (iron, chromium, tungsten, vanadium, molybdenum) by the depth of the layer of samples from R6M5 steel, treated by PPT in modes I and II, showed their uniform distribution that is indicative of the absence of additional alloying of the subsurface layers due to electrode material. Carbides of a complex composition of Me_6C type of a globular shape $(FeCr)_3(W, Mo)_3C$ with prevalence of tungsten and particle sizes $d_p \sim 0.21{-}2$ µm were found in the strengthened layer.

Transmission electron microscopy studies showed that base metal structure ($\delta > 100$ µm) is represented by tempering martensite with $\rho \leq 10^{11}$ cm^{-2}, residual austenite with $\rho \leq 10^{8}{-}10^{9}$ cm^{-2} and carbides (Figure 4).

In the layer of austenite grains ($\delta \leq 40$ µm) treated in mode I a coarsening of the substructure with formation of slightly disoriented block structure at overall non-uniformity of dislocation density ($\rho \sim 10^{8}{-}10^{9}$ cm^{-2}) is observed. In martensite of this zone an abrupt lowering of dislocation

density ($\rho \sim 10^{9}{-}10^{10}$ cm^{-2}) is noted compared to base metal martensite (Figure 5, *a*) that accounts for microhardness lowering (see Figure 3). The most dense ($\rho \sim (2{-}4) \cdot 10^{10}$ cm^{-2}) and extended ($l \sim 0.2{-}0.3$ µm) dislocation clusters form along contact boundaries of carbide phases and inner volumes of austenite grains, where $\rho \sim 10^{9}$ cm^{-2}.

In surface-melted layer 1 ($\delta \leq 5$ µm) increase of dimensions of substructural elements (blocks, cells) at their slight disorientation is observed, as well as non-uniform lowering of dislocation density at formation of abrupt gradients ($10^{8} \leq \rho \leq 10^{10}$ cm^{-2}) of dislocation density, i.e. stress raisers — zones of crack initiation and propagation (Figure 6, *a*). In the transition layer ($\delta \sim 40{-}100$ µm) with greater distance from sample surface, the tendency to lowering of dislocation density is preserved, but this lowering is not so significant compared to redistribution in PPT treated layer. Moreover, increase of micro-volumes with tempering structure (substructure, blocks) is observed that is in sharp contrast with base metal structure, which is characterized by finer-grain structure with dense and non-uniformly distributed dislocations.

Investigations of fine (dislocation) structure showed that PPT in mode II leads to higher dislocation density in the treated layer ($\delta \leq 40$ µm)

Figure 4. TEM-microstructure ($\times 20000$) of base metal of sample from R6M5 steel: *1* — carbides; *2* — residual austenite; *3* — tempering martensite
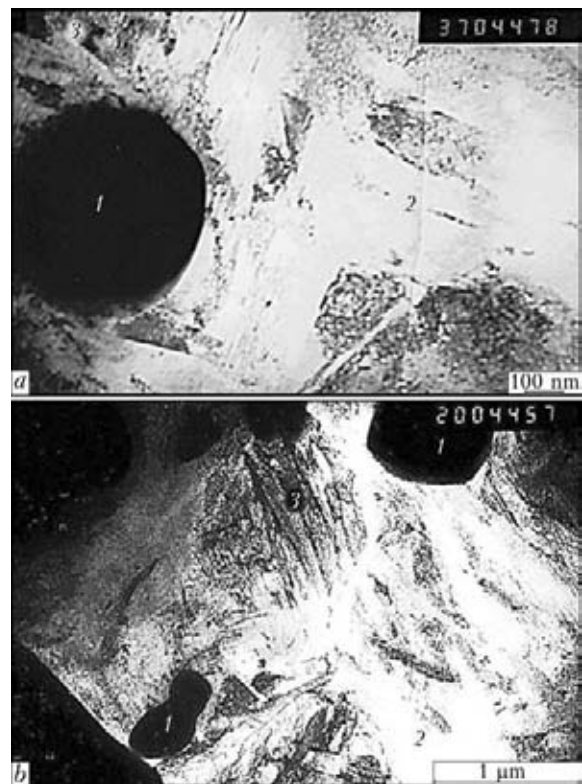
Figure 5. TEM-microstructure of surface layers of samples from steel R6M5 ($\delta = 5{-}40$ µm) after PPT in modes I (*a* — $\times 3700$) and II (*b* — $\times 20000$): *1* — carbides; *2* — residual austenite; *3* — martensite
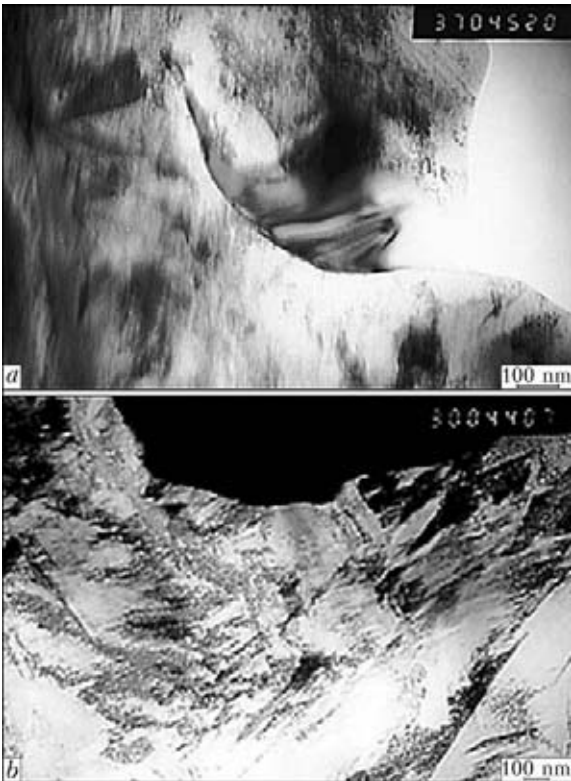
Figure 6. TEM-microstructure of surface layers of samples from steel R6M5 ($\delta \leq 5$ μm) after PPT in modes I (a — ×37000) and II (b — ×3000)

up to $\rho \leq 2 \cdot 10^{11}$ cm^{-2} in martensite compared to $\rho \leq 10^{11}$ cm^{-2} in the base metal (see Figures 4 and 5, b) that is in agreement with microhardness measurement results. For residual austenite grains a refinement of the substructure, formation of disoriented block structure are observed at overall uniformity of dislocation density ($\rho \sim 4 \cdot 10^9$ cm^{-2}). It is shown that martensite grains are also characterized by substructure refinement (lath width is 2 times smaller compared to base metal). With increase of the distance from the surface, a tendency to lowering of dislocation density and increase of microvolumes with tempering structure (substructure, blocks) is preserved.

Thus, it is established that in subsurface layers of R6M5 alloy structure refinement, increase of dislocation density and absence of extended dislocation clusters — sites of microcrack initiation and propagation — are found after PPT in mode II.

In order to assess the influence of PPT (various modes) on the most important service properties of working surfaces of tools from R6M5 steel, calculation-analytical evaluation of the properties of strength σ_y, fracture toughness K_{1c} and crack resistance $\tau_{l.in}/\tau_{theor}$ of modified steel layer was performed. It is established that after PPT in mode I leading to surface melting of the alloy surface layer, total $\Sigma\sigma_y$ level in the treated surface ($\delta \leq 40$ μm) decreases compared to the base metal by 50 % (640–940 MPa against 1330–1800 MPa
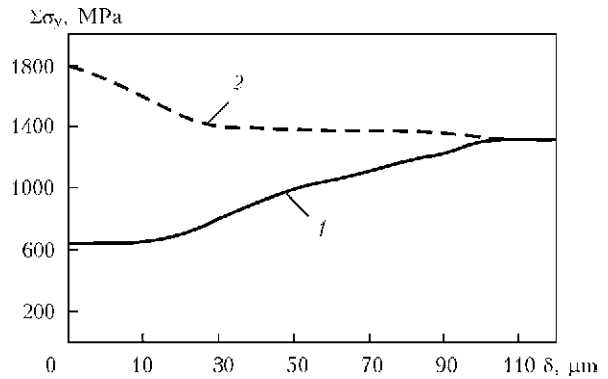
Figure 7. Change of average values of yield point $\Sigma\sigma_y$ by depth δ of treated layers of samples from steel R6M5 after PPT in modes I (*1*) and II (*2*)

in base metal) (Figure 7). The observed lowering of alloy strength in the surface layer is due to reduction of the contribution of substructural strengthening $\Delta\sigma_s \sim 190$–300 MPa compared to $\Delta\sigma_s \sim 590$–780 MPa in the base metal, grain strengthening $\Delta\sigma_{gr} \sim 200$–330 MPa compared to $\Delta\sigma_{gr} \sim 280$–480 MPa in the base metal, dislocation strengthening $\Delta\sigma_d \sim 20$–50 MPa compared to 200 MPa in the base metal. Therefore, softening in the alloy surface-melted layer (mode I, $\rho \sim 40$ μm) is due, predominantly, to the influence of coarsening of structure, and substructure, lowering of dislocations density and their non-uniform distribution.

At application of PPT mode II by treated layer depth ($\delta \sim 0$–40 μm) total strength level increases by 25 % (1400–2160 MPa at 1300–1800 MPa in the base metal). This is due to increased contribution of substructural ($\Delta\sigma_s \sim 490$–870 MPa), grain ($\Delta\sigma_{gr} \sim 440$–640 MPa), dislocation ($\Delta\sigma_d \sim 200$–283 MPa) strengthening, as well as strengthening due to dispersed particles ($\Delta\sigma_p \sim$
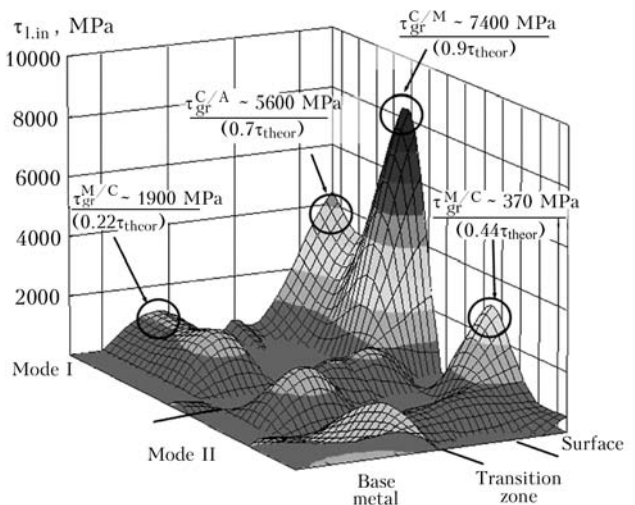
Figure 8. Level of local internal stresses $\tau_{l.in}$ in comparison with theoretical strength τ_{theor} in subsurface layers and in base metal of samples from R6M5 steel depending on PPT modes: C/M, C/A — interfaces of carbide–martensite and carbide–austenite structures, respectively
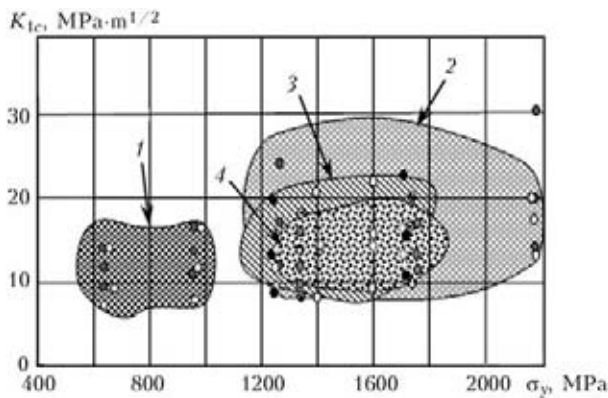
Figure 9. Change of strength σ_y and toughness K_{1c} of R6M5 steel by treated layer depth ($\delta \sim 0-100$ μm) after PPT in modes I and II compared to base metal: *1* — mode I; *2* — mode II; *3* — transition zone; *4* — base metal

$\sim 60-150$ MPa). This is also due to structure refinement, increase of total dislocation density, as well as realization of dispersion strengthening mechanism in the alloy subsurface layers.

Assessment of local inner stresses $\tau_{l.in}$ and their gradients $\Delta\tau_{in}$ along the structural component boundaries, the relationship of these values and theoretical strength of material by depth in the layer from PPT treated surface to base alloy R6M5 are given in Figure 8.

It is shown that after PPT of R6M5 alloy in mode I the highest $\tau_{l.in}$ values are found in the subsurface layers ($\delta \sim 0-40$ μm from outer surface) at the overall lowering of dislocations density and softening. These values form on interfaces of martensite/carbide (M/C) structures, being equal to $5600-7400$ MPa or $(0.67-0.90)\tau_{theor}$. Gradients of local internal stresses $\Delta\tau_{in}$ along the boundaries of these structural elements are equal to $5200-7000$ MPa and are potential crack initiation sources. After PPT in mode II, ρ increase (from 10^{11} up to $2\cdot10^{11}$ cm^{-2}) is observed compared to untreated alloy at comparatively uniform distribution of dislocation clusters that does not lead to formation of abrupt gradients of internal stresses $\Delta\tau_{l.in}$. This type of dislocation clusters correspond to value $\tau_{l.in} \sim 1480-3700$ MPa that is equal to $\sim 0.018-0.440$ of theoretical strength τ_{theor}. Here maximum $\tau_{l.in}$ values (~ 3700 MPa) are characteristic for M/C structure interfaces and do not create a risk of crack initiation.

Role of structural factors is manifested also in the change of strength of subsurface layers of tools from R6M5 alloys, namely properties of strength σ_y in combination with toughness characteristic K_{1c}, that is illustrated by the appropriate diagrams (Figure 9). It is found that K_{1c} value in the modified layer in mode I (with surface melting) is by 35 % lower than in mode II (without surface melting). Here, strength prop-

erties also decrease 1.8 times. After PPT in mode II, value K_{1c} in the modified layer of the alloy is by 15 % higher than in the base metal at a considerable strengthening of the entire layer.

Thus, proceeding from the conducted investigations and performed calculations it is established that application of mode II can be recommended for PPT of high-speed steel R6M5 as it leads to such structural-phase changes, which ensure a significant increase of the most important service properties, namely strength, ductility and crack resistance.

Conclusions

1. Pulsed-plasma treatment of samples from steel R6M5 using the mode of direct impact of pulsed electric discharge (mode I) leads to surface layer softening.

2. It is shown that in mode II total strength level increases up to $1400-2160$ MPa at $1300-1800$ MPa in the base metal across treated surface layer depth ($\delta \sim 0-40$ μm) that is due to the contribution of substructural ($\Delta\sigma_s \sim 490-\sim 870$ MPa), grain ($\Delta\sigma_{gr} \sim 440-640$ MPa), dislocation ($\Delta\sigma_d \sim 200-283$ MPa) strengthening mechanisms, as well as strengthening due to dispersed particles ($\Delta\sigma_p \sim 60-150$ MPa).

3. It is established that high level of strength and crack resistance (up to ~ 26 MPa·m$^{1/2}$) of surface layer of R6M5 steel after PPT in mode II is achieved at refinement ($D_{gr} \sim 1-5$ μm) of steel grain structure.

4. Pulsed-plasma treatment of samples with application of an indirect electric discharge (mode II) improves structural-phase state of modified layer and the set of its physico-mechanical properties, that is why mode II is the recommended mode for treatment of high-speed steel R6M5.

1. Mironov, V.M., Mazanko, V.F., Gertsriken, D.S. et al. (2001) *Mass transfer and phase formation under pulse effects*. Samara: Samara GU.
2. Burakov, V.V., Fedoseenko, S.S. (1983) Formation of structures of higher wear resistance in laser hardening of metal-working tools. *Metallovedenie i Term. Obrab. Metallov*, **5**, 16–17.
3. Volkhin, S.A. (1990) Influence of structure of tool steels after hardening and tempering on parameters of laser-hardened layers. *Sudostroit. Promyshlennost*, **23**, 44–48.
4. Sobusyak, T., Sokolov, K.N. (1991) Effect of laser heat treatment on structure and properties of high-speed steel. *Problemy Mashinostr. i Avtomatiz.*, **5**, 45–53.
5. Kikin, P.Yu., Pchelintsev, A.I., Rusin, E.E. (2003) Increase in heat- and wear resistance of high-speed steels by shock-wave action. *Fizika i Khimiya Obrab. Materialov*, **5**, 15–17.
6. Gureev, D.M., Lamtin, A.P., Chulkin, V.N. (1990) Influence of pulsed laser radiation on state of cobalt interlayer of hard alloys. *Ibid.*, **1**, 51–54.

7. Babushkin, V.B. (1990) Peculiarities of structure formation in high-speed and high-chromium die steels in laser heating. *Izvestiya Vuzov. Chyorn. Metallurgiya*, **4**, 68–70.
8. Markashova, L.I., Kolisnichenko, O.V., Valevich, M.L. et al. (2012) Structure and mechanical properties of tools from high-speed steel in pulse-plasma surface treatment. In: *Building, materials science, machine-building*: Transact. Issue 64, 211–220. Dnepropetrovsk: GVUZ PGASA.
9. Markashova, L.I., Tyurin, Yu.N., Kolisnichenko, O.V. et al. (2012) Analytical estimation of structural parameter contribution into change of mechanical properties of high-speed steel after pulse-plasma surface treatment. In: *Proc. of 6th Int. Conf. on Mathematical Modelling and Information Technologies in Welding and Related Processes*. Kiev: PWI, 49–53.
10. Cordier-Robert, C., Crampon, J., Foct, J. (1998) Surface alloying of iron by laser melting: Microstructure and mechanical properties. *Surface Eng.*, 14(**5**), 381–385.
11. Chudina, O.V., Borovskaya, T.M. (1994) Strengthening of steel surface by chemical-heat post treatment. *Metallovedenie i Term. Obrab. Metallov*, **12**, 2–7.
12. Chudina, O.V. (1997) Surface alloying of iron-carbon alloys with application of laser heating. *Ibid.*, **7**, 11–14.
13. Ritter, U., Kahrmann, W., Kurpfer, R. et al. (1992) Laser coating proven in practice. *Surface Eng.*, 8(**4**), 381–385.
14. Lugscheider, E., Boplender, H., Krappitz, H. (1992) Laser cladding of paste bound hardfacing alloys. *Ibid.*, 7(**4**), 341–344.
15. Navara, E., Bengsston, B., Li, W.B. et al. (1984) Surface treatment of steel by laser transformation hardening. In: *Proc. of 3rd Int. Congr. on Heat Treatment of Materials* (Shanghai, 7–11 Nov. 1983). Shangri: Metal Society, 40–44.
16. Tverdokhlebov, T.N., Diachenko, V.S. (1980) Influence of laser treatment conditions on resistance of high-speed steel tools. In: *Cutting equipment and tools*. Moscow: Mashinostroenie.
17. Hancock, I.M. et al. (1988) Laser modification of high-speed steel. In: *Proc. of Int. Conf. on Heat Treatment* (London, 11–15 May 1987). London: Metal Society, 189–195.
18. Tyurin, Yu.N., Zhadkevich, M.L. (2008) *Plasma hardening technologies*. Kiev: Naukova Dumka.
19. Suzuki, H. (1967) About yield strength of polycrystalline metals and alloys. In: *Structure and mechanical properties of metals*. Moscow: Metallurgiya.
20. Eshby, M.F. (1972) On Orowan stress. In: *Physics of strength and plasticity*. Moscow: Metallurgiya.
21. Goldshtejn, M.I., Litvinov, V.S., Bronfin, B.M. (1986) *Metallophysics of high-strength alloys*. Moscow: Metallurgiya.
22. Conrad, H. (1973) Model of strain hardening for explanation of size grain effect on flow metal stress. In: *Ultrafine grains in metals*. Ed. by L.K. Gordienko. Moscow: Metallurgiya.
23. Armstrong, R.V. (1973) Strength properties of metals with ultrafine grains. *Ibid*. Moscow: Metallurgiya.
24. Petch, N.J. (1953) The cleavage strength of polycrystalline. *J. Iron and Steel Inst.*, 173(**1**), 25–28.
25. Orowan, E. (1954) *Dislocation in metals*. New York: AIME.
26. Ashby, M.F. (1983) Mechanisms of deformation and fracture. *Adv. Appl. Mech.*, **23**, 118–177.
27. Kelly, A., Nickolson, R. (1966) *Dispersion hardening*. Moscow: Metallurgiya.
28. Ebelling, R., Ashby, M.F. (1966) Yielding and flow of two phase copper alloys. *Phil. Mag.*, 13(**7**), 805–809.
29. Romaniv, O.N. (1979) *Fracture toughness of structural steels*. Moscow: Metallurgiya.
30. Koneva, N.A., Lychagin, D.V., Teplyakova, L.A. et al. (1986) Dislocation-disclination substructures and hardening. In: *Theoretical and experimental study of disclinations*. Leningrad: LFTI.
31. Conrad, H. (1963) Effect of grain size on the lower yield and flow stress of iron and steel. *Acta Met.*, **11**, 75–77.